JSIAM Letters Vol.11 (2019) pp.29–32 ©2019 Japan Society for Industrial and Applied Mathematics

Reconstruction of current dipoles based on tensor decomposition of multipole coefficients

Kenta Kabashima[1], Tianxiong Wu[1] and Takaaki Nara[1]

[1] The University of Tokyo, 7-3-1 Hongo, Bunkyo, Tokyo 113-8656, Japan

E-mail *kenta_program37@hotmail.co.jp*

Received December 04, 2018, Accepted January 15, 2019

Abstract

This paper presents a novel method for solving magnetoencephalography (MEG) inverse problems using the CANDECOMP/PARAFAC decomposition of a tensor in which Hankel matrices composed of the multipole moments of the observed data are aligned. The proposed method can reconstruct the positions and moments of the current dipoles in the human brain projected on the xy-plane more stably than the conventional direct method using Prony's algorithm. A novel spherical-spline-based method for the computation of the multipole moments is also proposed.

Keywords current dipole, multipole expansion, CANDECOMP/PARAFAC decomposition

Research Activity Group Algorithms for Matrix / Eigenvalue Problems and their Applications

1. Introduction

Magnetoencephalography (MEG) is the measurement of the magnetic flux density on the surface of a human's head, and is used to estimate the current sources in the brain. The methods for solving the inverse problems can be classified into linear and non-linear methods. The imaging method in [1] is a typical linear method, in which the current sources fixed on the grids for the cerebral cortex are obtained by solving a system of linear equations. The non-linear methods are further classified into optimization-based methods and direct methods. They determine the positions, moments, and number of multiple current dipoles via non-linear optimization or direct algorithms. In the direct method in [2], a system of algebraic equations between the dipoles projected on the xy-plane and the multipole coefficients of the single-time-shot magnetic flux density data is solved using the so-called Prony method. However, such a reconstruction with each time-shot data has the problem of not being able to stably detect the onset of a dipole. An example is shown in Fig. 2. Another significant source of errors is the truncation of the multipole expansion. The multipole coefficients used in the Prony method are usually computed with equations obtained by truncating the infinite series in the multipole expansion, and the order of the truncation affects the reconstruction accuracy. To resolve these problems, we first propose the composition of a 3rd-order tensor in which the time-series of the Hankel matrices used in the conventional method are aligned, and then apply CANDECOMP/PARAFAC (CP) decomposition [3] to it to stably obtain the dipole parameters. Second, we propose a method to compute multipole coefficients to reduce the effect of the truncation order using an extended spherical spline for MEG sensors.

The rest of the paper is organized as follows. In Section 2, we summarize the forward and inverse problems and introduce the multipole coefficients. In Section 3, CP decomposition and its algorithm are introduced for the reconstruction of dipole parameters from the time-series of the multipole coefficients. In Section 4, an extended spherical spline for MEG sensors is derived for the calculation of the multipole coefficients. The results of numerical experiments are shown in Section 5.

Notation For a complex matrix $A \in \mathbb{C}^{m\times n}$, A^* denotes the adjoint of A, and $A^\dagger$ denotes the Moore-Penrose's generalized inverse of A. In this paper, the term "tensor" refers to a multi-dimensional array, as in [3], with its elements denoted by subscripts as x_{ijk}, and superscripts representing not indices of elements but exponents of powers. For a complex tensor $\mathcal{X}$, its norm $\|\mathcal{X}\|_F$ is defined as the sum of the squared absolute values of elements, just like the Frobenius' norm of a matrix.

2. Forward and inverse problem

First, we summarize the MEG forward and inverse problems. Assuming that a head consists of concentric spheres [4], the current dipoles $\boldsymbol{p}_n$ at positions $\boldsymbol{r}_n = (x_n, y_n, z_n)^\top \in \Omega$ $(n = 1, 2, \dots, N)$, where Ω represents a brain, generate a magnetic flux density outside the head as follows [4]:

$$\boldsymbol{B}(\boldsymbol{r}, t) = \sum_{n=1}^{N} \frac{\mu_0}{4\pi F^2}(F\boldsymbol{p}_n \times \boldsymbol{r}_n - \boldsymbol{p}_n \times \boldsymbol{r}_n \cdot \boldsymbol{r}\nabla F), \quad (1)$$

where μ_0 is the permeability of the free space, $F = a(ra + \boldsymbol{a}\cdot\boldsymbol{r})$, $\boldsymbol{a} = \boldsymbol{r} - \boldsymbol{r}_n$, and $a = \|\boldsymbol{a}\|_2$. This is the forward solution. The inverse problem involves identifying the dipole parameters from the time-series measurements of $\boldsymbol{B}(\boldsymbol{r}, t)$ at the sensor positions.

It is well known that the magnetic flux density can be expressed by the multipole expansion as follows [5]:

$$\boldsymbol{B}(\boldsymbol{r},t) = -\mu_0 \sum_{l=1}^{\infty} \sum_{m=-l}^{l} \frac{M_{lm}(t)}{2l+1} \nabla \frac{\overline{Y_{lm}(\theta,\varphi)}}{r^{l+1}}, \tag{2}$$

where (r,θ,φ) are the spherical coordinates of point $\boldsymbol{r}$, M_{lm} are the multipole coefficients, and $Y_{lm}(\theta,\varphi)$ are (normalized) spherical harmonics ([6]). Here, it is shown that the multipole moments for $l = m$ are expressed in terms of the dipole parameters as follows [2]:

$$\begin{aligned} \alpha_k(t) &\equiv -\frac{1}{\mu_0}\frac{k+2}{k+1}\sqrt{\frac{4\pi}{2k+3}\frac{(2k+2)!!}{(2k+1)!!}}\, M_{k+1,k+1}(t) \\ &= \sum_{n=1}^{N} m_n(t) s_n^k, \end{aligned} \tag{3}$$

where $\boldsymbol{m}_n(t) \equiv \boldsymbol{r}_n \times \boldsymbol{p}_n(t) \equiv (m_{xn}, m_{yn}, m_{zn})^\top$ is the magnetic moment of the nth dipole, and $s_n = x_n + iy_n$ and $m_n(t) = m_{xn} + im_{yn}$ are projections on the xy-plane of $\boldsymbol{r}_n$ and $\boldsymbol{m}_n(t)$, respectively. Hence, solving (3) for $m_n(t)$ and s_n using the value of $\alpha_k(t)$ computed from the magnetic field data provides a solution to the inverse problem. In fact, (3) can be solved for $m_n(t)$ and s_n using $\alpha_k(t)$ for $k = 0, 1, \ldots, 2N-1$ using Prony method [2]. Note here that all the parameters are determined from a single time-shot of the multipole moments $\alpha_k(t)$. (The z components of the dipole positions and moments are also algebraically identified.) However, a problem of this method is that the reconstructed dipole positions are scattered, especially at the onset of dipole moments, as shown in numerical simulations in Section 5.

3. CP decomposition

In this paper, we propose the use of the time sequence of $\alpha_k(t)$ to enhance the estimation stability of the dipole parameters. Because our primary goal is detecting the onset of dipoles in a short duration, we assume that the positions of the dipoles are fixed while their moments change with respect to time.

For this purpose, we align $\alpha_k(t)$ in a tensor $\mathcal{X} \in \mathbb{C}^{N\times N\times T}$ such that the (i,j,k) element is given by $x_{ijk} = \alpha_{i+j-2}(t_k)$, where t_k is the kth sampling time. Then, from (3), we have the following:

$$x_{ijk} = \sum_{n=1}^{N} s_n^{i-1} s_n^{j-1} m_n(t_k). \tag{4}$$

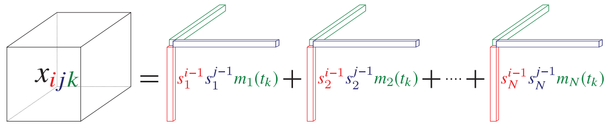

Fig. 1. Schematic description of (4).

This shows that s_n and $m_n(t_k)$ can be obtained by CP decomposition [3] of tensor $\mathcal{X}$, as in Fig. 1. Here, for a tensor $\mathcal{X} \in \mathbb{C}^{I\times J\times K}$, a decomposition

$$x_{ijk} = \sum_{r=1}^{R} a_{ir} b_{jr} c_{kr},$$

which is denoted as $\mathcal{X} = [\![A,B,C]\!]$, can be computed using an alternating least squares (ALS) algorithm. It minimizes the residual $\|\mathcal{X} - [\![A,B,C]\!]\|_F$ by repeatedly solving linear equations as follows:

(i) calculate A, which minimizes the residual for fixed B and C;

(ii) calculate B, which minimizes the residual for fixed A and C, and

(iii) calculate C, which minimizes the residual for fixed A and B.

Following derivation of a solution for a real tensor in [3], it is easy to obtain a solution for a complex tensor as follows:

$$\begin{aligned} A^\top &= [(C^*C) * (B^*B)]^\dagger (C \odot B)^* {X_{(1)}}^\top, \\ B^\top &= [(C^*C) * (A^*A)]^\dagger (C \odot A)^* {X_{(2)}}^\top, \\ C^\top &= [(B^*B) * (A^*A)]^\dagger (B \odot A)^* {X_{(3)}}^\top. \end{aligned}$$

Here, $A \odot B$ for $A \in \mathbb{C}^{l\times n}$ and $B \in \mathbb{C}^{m\times n}$ denotes the Khatri-Rao product, $A * B$ for A and $B \in \mathbb{C}^{m\times n}$ denotes the Hadamard product, and $X_{(i)}$ are the matricizations of $\mathcal{X}$.

In this way, using the time series of $\alpha_k(t)$ and solving the linear equations iteratively, we obtain the xy-projection of the positions and moments.

4. Spherical spline

In this section, we develop an extended spherical spline for MEG sensors to reduce the effect of the truncation order when computing the multipole moments used in the CP decomposition described in Section 3.

We define a function f as the magnetic flux density at point $\boldsymbol{r}$ for direction $\boldsymbol{n}$:

$$f(\boldsymbol{r},\boldsymbol{n}) \equiv -\mu_0 \sum_{l=1}^{\infty}\sum_{m=-l}^{l} \frac{M_{lm}}{2l+1} \boldsymbol{n}\cdot\nabla \frac{\overline{Y_{lm}(\theta,\varphi)}}{r^{l+1}}. \tag{5}$$

Note here that f and M_{lm} depend on time t, although it is omitted for simplicity. Two kinds of sensors are used in MEG: a magnetometer, which measures the magnetic flux density $f_i \equiv f(\boldsymbol{r}_i, \boldsymbol{n}_i)$, where $\boldsymbol{r}_i$ is the ith sensor position and $\boldsymbol{n}_i$ is the unit normal vector of the sensor coil, and a gradiometer which measures the difference $f_i \equiv f(\boldsymbol{r}_{i1}, \boldsymbol{n}_i) - f(\boldsymbol{r}_{i2}, \boldsymbol{n}_i)$ for two points $\boldsymbol{r}_{i1}$, $\boldsymbol{r}_{i2}$ and a direction $\boldsymbol{n}_i$. Let us express them in a unified manner as follows:

$$f_i = L_i[f(\boldsymbol{r},\boldsymbol{n})] \equiv \sum_{j=1}^{s_i} c_{ij} f(\boldsymbol{r}_{ij}, \boldsymbol{n}_{ij}), \tag{6}$$

where L_i is an operator applied to $f(\boldsymbol{r},\boldsymbol{n})$. When the ith sensor is a magnetometer, $s_i = 1$, $c_{i1} = 1$, $\boldsymbol{r}_{i1} = \boldsymbol{r}_i$, and $\boldsymbol{n}_{i1} = \boldsymbol{n}_i$; when the ith sensor is a gradiometer, $s_i = 2$, $c_{i1} = 1$, and $c_{i2} = -1$.

We need to estimate the multipole coefficients M_{lm} from a finite number of data points. For that purpose, let us truncate the infinite series (5) up to $l = l_{\max}$ and determine M_{lm} for $l \le l_{\max}$ from f_i $(i = 1, 2, \ldots, M)$. Set $\mathrm{ind}(l,m) \equiv l(l+1)+m$ and define a vector $\boldsymbol{u}$ of dimension $(l_{\max}+1)^2$ whose $\mathrm{ind}(l,m)$-th component is given by

$u_{\mathrm{ind}(l,m)} = M_{lm}$. Let us also define an $M \times (l_{\max}+1)^2$ matrix as follows:

$$A_{i,\mathrm{ind}(l,m)} = -\mu_0 \frac{1}{2l+1} L_i \left[\boldsymbol{n} \cdot \nabla \frac{\overline{Y_{lm}(\theta,\varphi)}}{r^{l+1}} \right], \tag{7}$$

as well as an M-dimensional data vector $\boldsymbol{f} = (f_1, f_2, \ldots, f_M)^\top$. Taulu *et al.* [7] proposed the minimization of $\|A\boldsymbol{u} - \boldsymbol{f}\|_2^2$ to obtain $\boldsymbol{u}$ in the truncated multipole expansion. In this method, the linear equation to be solved becomes under-determined if $l_{\max}$ increases. In order to obtain a unique solution when $(l_{\max}+1)^2 > M$, we here consider the minimization problem:

$$J_d(\boldsymbol{u}) = \|A\boldsymbol{u} - \boldsymbol{f}\|_2^2 + \lambda R \tag{8}$$

where R is a regularization term defined by

$$R \equiv \int_{S_0} \left| \triangle_{\theta,\varphi}^{\frac{d}{2}} f(\boldsymbol{r}, \boldsymbol{n}_r) \right|^2 dS = \|D\boldsymbol{u}\|_2^2, \tag{9}$$

and $\lambda > 0$ is a regularization parameter. Here, S_0 is a sphere centered at the origin with radius r_0, $\triangle_{\theta,\varphi}$ is the surface Laplacian on the sphere S_0 given by

$$\triangle_{\theta,\varphi} \equiv \frac{1}{r^2 \sin\theta} \frac{\partial}{\partial\theta} \left(\sin\theta \frac{\partial}{\partial\theta} \right) + \frac{1}{r^2 \sin^2\theta} \frac{\partial^2}{\partial\varphi^2}, \tag{10}$$

d is an even number, $\boldsymbol{n}_r$ is a unit vector $\boldsymbol{r}/\|\boldsymbol{r}\|_2$, and the coefficient matrix D is a diagonal matrix defined as

$$D_{\mathrm{ind}(l,m),\mathrm{ind}(l,m)} = \frac{\mu_0 l^{\frac{d}{2}} (l+1)^{\frac{d}{2}+1}}{r_0^{l+1}(2l+1)}. \tag{11}$$

With this regularization term, the optimal solution can be written as follows:

$$\boldsymbol{u} = \left(A^* A + \lambda D^2 \right)^{-1} A^* \boldsymbol{f}. \tag{12}$$

Now, we transform this expression as follows:

$$\boldsymbol{u} = D^{-2} A^* \left(A D^{-2} A^* + \lambda I \right)^{-1} \boldsymbol{f}, \tag{13}$$

and introduce a variable $\boldsymbol{c}$ by

$$\boldsymbol{u} = D^{-2} A^* \boldsymbol{c} \tag{14}$$

where $\boldsymbol{c}$ satisfies

$$\left(A D^{-2} A^* + \lambda I \right) \boldsymbol{c} = \boldsymbol{f}. \tag{15}$$

Note here that $AD^{-2}A^* + \lambda I$ is a non-singular square matrix even if $(l_{\max}+1)^2 > M$. Hence, by solving the well-determined equation (15) for $\boldsymbol{c}$ and substituting the result into (14), we can determine $\boldsymbol{u}$ even when $(l_{\max}+1)^2 \gg M$. The result is summarized as follows.

Theorem 1 *The regularized optimal solution of $M_{lm} = u_{\mathrm{ind}(l,m)}$ can be expressed as*

$$M_{lm} = -\frac{r_0^{2l+2}(2l+1)}{\mu_0 l^d (l+1)^{d+2}} \sum_{i=1}^{M} c_i L_i \left[\boldsymbol{n} \cdot \nabla \frac{Y_{lm}(\theta,\varphi)}{r^{l+1}} \right], \tag{16}$$

where c_i can be obtained by solving a linear equation

$$(K + \lambda I)\boldsymbol{c} = \boldsymbol{f} \tag{17}$$

with a coefficient matrix $K_{ij} \equiv L_i[L'_j[K_1(\boldsymbol{r}, \boldsymbol{n}, \boldsymbol{r}', \boldsymbol{n}')]]$. The kernel function K_1 is given by

$$\begin{aligned} K_1(\boldsymbol{r}, \boldsymbol{n}, \boldsymbol{r}', \boldsymbol{n}') &\equiv \sum_{l=1}^{l_{max}} \sum_{m=-l}^{l} \frac{r_0^{2l+2}}{l^d (l+1)^{d+2}} \\ &\quad \boldsymbol{n} \cdot \nabla \frac{\overline{Y_{lm}(\theta,\varphi)}}{r^{l+1}} \boldsymbol{n}' \cdot \nabla' \frac{Y_{lm}(\theta,\varphi)}{r'^{l+1}} \qquad (18) \\ &= \sum_{l=1}^{l_{max}} \frac{2l+1}{4\pi l^d (l+1)^{d+2}} (\boldsymbol{n} \cdot \nabla)(\boldsymbol{n}' \cdot \nabla') \\ &\quad \left[\left(\frac{r_0}{r} \right)^{l+1} \left(\frac{r_0}{r'} \right)^{l+1} P_l(\cos\omega) \right], \qquad (19) \end{aligned}$$

where ω is the angle between two vectors $\boldsymbol{r}$ and $\boldsymbol{r}'$.

Note here that L_i and L'_j are applied to an arbitrary function $g(\boldsymbol{r}, \boldsymbol{n}, \boldsymbol{r}', \boldsymbol{n}')$ as follows:

$$L_i[g(\boldsymbol{r}, \boldsymbol{n}, \boldsymbol{r}', \boldsymbol{n}')] \equiv \sum_{j=1}^{s_i} c_{ij} g(\boldsymbol{r}_{ij}, \boldsymbol{n}_{ij}, \boldsymbol{r}', \boldsymbol{n}'),$$

$$L'_i[g(\boldsymbol{r}, \boldsymbol{n}, \boldsymbol{r}', \boldsymbol{n}')] \equiv \sum_{j=1}^{s_i} c_{ij} g(\boldsymbol{r}, \boldsymbol{n}, \boldsymbol{r}_{ij}, \boldsymbol{n}_{ij}).$$

Corollary 2 *Using c_i in (17), the magnetic flux density can be interpolated using the following function:*

$$\hat{f}(\boldsymbol{r}, \boldsymbol{n}) \equiv \sum_{i=1}^{M} c_i L'_i K_1(\boldsymbol{r}, \boldsymbol{n}, \boldsymbol{r}', \boldsymbol{n}'). \tag{20}$$

Remark 3 This result is an extension of the spherical spline derived in [8] for interpolating functions on spheres, where the following objective functional for the interpolation was defined:

$$J_d[f] \equiv \sum_{i=1}^{M} |f(\boldsymbol{r}_i) - f_i|^2 + \lambda \int_S \left| \triangle_{\theta,\varphi}^{\frac{d}{2}} f(\boldsymbol{r}) \right|^2 dS, \tag{21}$$

and the optimal solution was found as follows

$$\hat{f}(\boldsymbol{r}) = \sum_{i=1}^{M} c_i K_1(\boldsymbol{r}, \boldsymbol{r}_i) + c_0, \tag{22}$$

$$K_1(\boldsymbol{r}, \boldsymbol{r}') \equiv \sum_{l=1}^{\infty} \sum_{m=-l}^{l} \frac{1}{[l(l+1)]^d} Y_{lm}(\boldsymbol{r}) \overline{Y_{lm}(\boldsymbol{r}')}. \tag{23}$$

However, (21) through (23) cannot be directly used for MEG inverse problems for the following reasons. (i) Gradiometers measure the difference between the magnetic flux densities at two points, not a scalar at a single point. (ii) The scalar data are determined by the magnetic field and the coil's normal. (iii) All of the sensors do not exist on a single sphere. To solve all of these problems, we defined the objective functional as follows:

$$J_d[f] \equiv \sum_{i=1}^{M} |L_i f(\boldsymbol{r}, \boldsymbol{n}) - f_i|^2 + \lambda \int_{S_0} \left| \triangle_{\theta,\varphi}^{\frac{d}{2}} f(\boldsymbol{r}, \boldsymbol{n}_r) \right|^2 dS.$$

Note that with the assumption that r_0 is small and thus all the sensors are outside the sphere S_0, Theorem 1 and Corollary 2 can be proven, even under the condition $l_{\max} \to \infty$, based on the theory of reproducing kernel Hilbert spaces, as in [8].

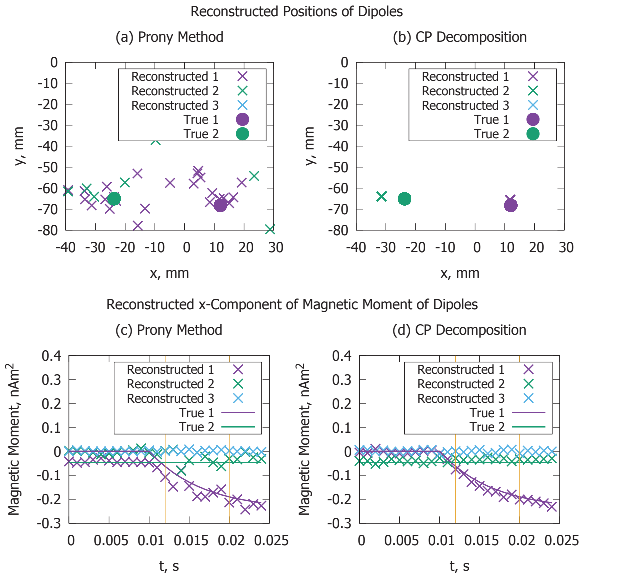

Fig. 2. Simulations of two dipoles whose time-series of moments are given in (c) and (d), positions reconstructed using Prony method scattered as in (a), whereas the proposed method stably identified true positions as in (b).

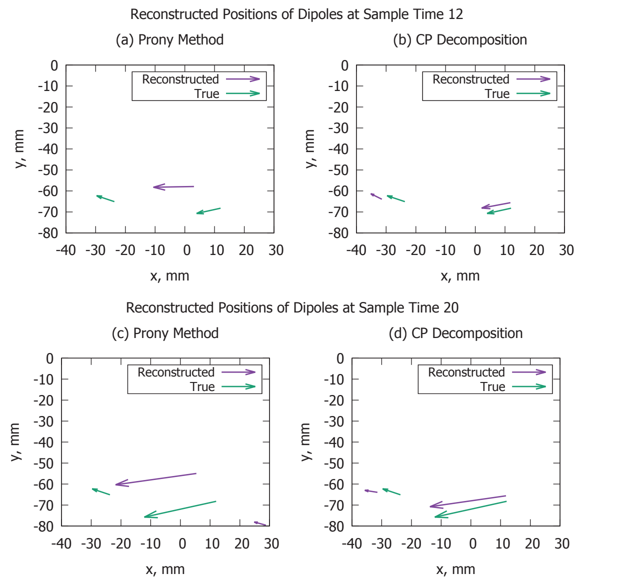

Fig. 3. Positions and moments of dipoles reconstructed using Prony method and CP decomposition at 12 ms and 20 ms (source: 2 dipoles, reconstruction: 3 dipoles).

5. Numerical experiments

A numerical comparison was made of the proposed method and Prony method. We assumed two dipoles ($N = 2$): one had a constant weak moment and the other started to be active at 10 ms, as in Fig. 2 (c). The MEG data were calculated using (1), with 5% Gaussian noise added to the data. A total of 306 sensors was assumed, as in an Elekta Neuromag device. We computed the multipole moments using (16) and (17), where $d = 0$. Kahan's algorithm [9] was used to determine $l_{\max}$ such that the right hand side of (19) did not change if $l_{\max}$ was increased. $l_{\max}$ depended on i and j when computing K_{ij} and ranged from 47 to 172. The regularization parameter λ was computed with L-curve criterion [10]. Because the number of dipoles N is not known *a priori*, we assumed that there existed $N' = 3$ dipoles. The number of sample points, T, was 25.

Figs. 2 (a)/(b) and (c)/(d) show the positions and moments reconstructed by the Prony/proposed methods, respectively. The estimated positions were scattered by the Prony method, as in Fig. 2 (a), whereas our method stably identified the true positions, as in Fig. 2 (b). In Fig. 2 (c), we observe that a weak dipole ("True 2" in the figures) could be correctly estimated only before the onset of the other dipole ("True 1") by the Prony method. In fact, at 12 ms around the onset of the True 1 dipole, the Prony method localized a single dipole between two dipoles, as in Fig. 3 (a). At 20 ms, a single dipole was estimated, as in Fig. 3 (c). In contrast, our method stably estimated two dipoles at both time as in Fig. 3 (b) and (d). Note also that the moment of the third dipole was smaller than those of the first two dipoles in Fig. 2 (d), and hence N could be estimated by our method.

6. Conclusion

In this study, we applied CP decomposition to a tensor in which a time-series of Hankel matrices composed of the multipole coefficients were aligned and showed numerically that the proposed method could reconstruct dipole parameters more stably than the Prony method. In addition, we extended a spherical spline for MEG sensors and verified that the multipole coefficients estimated by it could be used for the reconstruction of dipole parameters.

Acknowledgement

This work was partially supported by JST PRESTO.

References

[1] Y. Petrov, Harmony: EEG/MEG linear inverse source reconstruction in the anatomical basis of spherical harmonics, PLoS ONE, **7** (2012), 1–15.
[2] T. Nara, J. Oohama, M. Hashimoto, T. Takeda and S. Ando, Direct reconstruction algorithm of current dipoles for vector magnetoencephalography and electroencephalography, Phys. Med. Biol., **52** (2007), 3859–3879.
[3] T. G. Kolda and B. W. Bader, Tensor decompositions and applications, SIAM Rev., **51** (2008), 455–500.
[4] M. Hämäläinen, R. Hari, R. J. Ilmoniemi, J. Knuutila and O. V. Lounasmaa, Magnetoencephalography—theory, instrumentation, and applications to noninvasive studies of the working human brain, Rev. Modern Phys., **65** (1993), 413–497.
[5] K. Jerbi, J. C. Mosher, S. Baillet and R. M. Leahy, On MEG forward modelling using multipolar expansions, Phys. Med. Biol., **47** (2002), 523–555.
[6] P. M. Morse and H. Feshbach, Methods of Theoretical Physics, McGraw-Hill, New York, 1953.
[7] S. Taulu and M. Kajola, Presentation of electromagnetic multichannel data: The signal space separation method, J. Appl. Phys., **97** (2005), 1–10.
[8] G. Wahba, Spline interpolation and smoothing on the sphere, SIAM J. Sci. Comput., **2** (1981), 5–16.
[9] W. Kahan, Further remarks on reducing truncation errors, Commun. ACM, **8** (1965), 40.
[10] P. C. Hansen, Rank-Deficient and Discrete Ill-Posed Problems: Numerical Aspects of Linear Inversion, SIAM, Philadelphia, 1998.